Univerzita Karlova v Praze
Matematicko-fyzikální fakulta

BAKALÁŘSKÁ PRÁCE

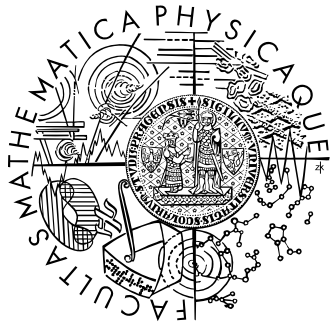

Martin Rusňák

Strukturní nespojitost v systému RTX

Katedra fyziky kondenzovaných látek

Vedoucí bakalářské práce: RNDr. Jiří Prchal, Ph.D.

Studijní program: Obecná fyzika

2008

Univerzita Karlova v Praze
Matematicko-fyzikální fakulta

BACHELOR THESIS

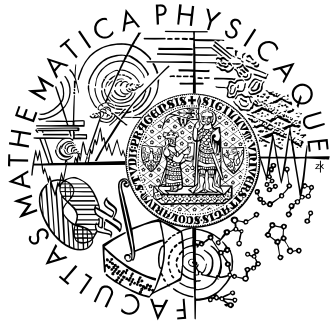

Martin Rusňák

Structure discontinuity in the RTX ternary system

Department of condensed matter physics

Supervisor: RNDr. Jiří Prchal, Ph.D.

Study programme: General physics

2008

I would like to thank to supervisor of my work RNDr. Jiří Prchal, Ph.D., under whose supervising this thesis was created, RNDr. Stanislav Daniš, Ph.D, for useful consultations and advices, and to everybody who helped me with this work. Once more I would like to expres my gratitude to RNDr. Stanislavov Daniš, Ph.D and Jan Matlák for their work on preparation of the aparature.

I claim that I have written my work on my own and only with use of the referenced literature. I agree with lending of the thesis and its publicating.

V Prahe dňa 26. 5. 2008 Martin Rusňák

Content

Názov práce: Strukturní nespojitost v ternárním systému RTX

Autor: Martin Rusňák

Katedra: Katedra fyziky kondenzovaných látek

Vedúci bakalárskej práce: RNDr. Jiří Prchal, Ph.D.

e-mail vedúceho: prchal@karlov.mff.cuni.cz

Abstrakt: $Ce_{1-x}Y_xPdAl$ patrí do skupiny hexagonálnych RTX zlúčenin (R značí vzácnu zeminu, T tranzitný kov, X p-kov). Tri vzorky so zložením x= 0,2, 0,5 a 0,8 sme študovali použitím röntgenovej difrakcie pri izbovej teplote. Bolo pozorované nezvyčajné správanie sa mriežkových parametrov a, c a ich vzájomného pomeru c/a pri zmene substitúcie x. Bola potvrdená existencia oblasti zakázaných hodnôt pomeru c/a. Pre x = 0,2 a 0,8 je zlúčenina jednofázová, pričom obe fázy sa líšia pomerom c/a. Pre x= 0,5 zlúčenina vykazuje koexistenciu oboch x=0,2 a 0,8 fáz.

Okrem toho sme skúmali správanie vzorku $Ce_{0,5}Y_{0,5}PdAl$ v teplotnom rozsahu od 300K do 500K. Na základe získaných difrakčných vzorov a mriežkových parametrov tvrdíme, že $Ce_{0,5}Y_{0,5}PdAl$ vzorok vykoná fázový prechod z dvojfázového systému pri izbovej teplote do jednofázového pri vyšších teplotách.

Kľúčové slová: CeYPdAl, RTX, röntgenová difrakcia, štruktúra typu ZrNiAl, zakázané hodnoty pomeru c/a

Title: Structure discontinuity in the RTX ternary system

Author: Martin Rusňák

Department: Department of condensed matter physics

Supervisor: RNDr. Jiří Prchal, Ph.D.

Supervisor's e-mail adress: prchal@karlov.mff.cuni.cz

Abstract: The $Ce_{1-x}Y_xPdAl$ pseudoternaries belong to ternary RTX compounds (where R stands for rare-earth, T for transition metal, X for p-metal). We have studied three samples with composition x = 0.2, 0.5 and 0.8 by means of X-ray diffraction technique at room temperature. An anomalous evolution of lattice parameters (a, c) and their ratio (c/a) was observed at room temperature with change in substitution parameter x. Existence of gap of forbidden values of c/a ratio was confirmed. For x = 0.2 and 0.8 the compound is in different single phases. For x = 0.5 the compound exhibits coexistence of both the x = 0.2 and x=0.8 phases.

Moreover, the $Ce_{0.5}Y_{0.5}PdAl$ compound was studied also in the temperature range from 300K to 500K. According to obtained diffraction patterns and calculated lattice parameters obtained from the $Ce_{0.5}Y_{0.5}PdAl$ high temperature diffraction experiment we state that the sample undergoes a phase transition towards the single phased state at higher temperatures.

Key-words: CeYPdAl; X-ray diffraction; ZrNiAl-type structure; Forbidden c/a ratio

1 Motivation

The ternary RTX compounds (where R stands for rare-earth, T for transition metal, X for p-metal), belong to a large group of 1:1:1 compounds. They may crystallize in many variations, but the most common are the orthorhombic TiNiSi-type structure, the hexagonal AlB_2-type structure, and the hexagonal ZrNiAl-type structure. They exhibit interesting electric and magnetic properties [1-7]. While investigating these properties an unusual structural behaviour was observed [1,3,8-12]. With varying temperature or composition (substitution Ni-Cu, Ni-Pd), there was observed an evolution of the c/a ratio with a gap of forbidden values in range from 0.565 to 0.575. According to the c/a ratio the compounds are either in the “low c/a” (below 0.565) or in the “high c/a” (above 0.575) phase. Transition from one phase to other one is connected with coexistence of both of the phases.

Previously mentioned substitutions were on the position of the transition metal element. $Ce_{1-x}Y_xPdAl$ is first type of compound with substitution on the rare-earth element position, which exhibits similar type of structural transition [13]. Unlike the other ones in this series the c/a ratio fall into the forbidden range, nevertheless other aspects of the transition are similar. Aim of this work is to investigate lattice parameters evolution of the $Ce_{1-x}Y_xPdAl$ in dependence on temperature.

2 Theory

2.1 Crystal structure

Crystal structure is a unique arrangement of atoms in a crystal. A crystal structure is made of a motif and a lattice. Motifs are located upon the lattice. Lattice is an array of points periodically repeated in three dimensions. The smallest set of points from which the array can be built and that determines all the symmetry properties of the whole array is called unit cell. The lengths of the edges of a unit cell and the angles between them are called the lattice parameters. According to the symmetry of the lattice, we divide crystals into 230 space groups. Many of the physical properties such as cleavage, electronic band structure, and optical properties are determined by the structure and symmetry of the crystal.

2.2 ZrNiAl-type structure

Our studied materials belong to the group of ternary intermetallic RTX compounds crystallizing in ZrNiAl-type hexagonal structure (space group P-62m ; group No. 189; see Figure 2.2.1).

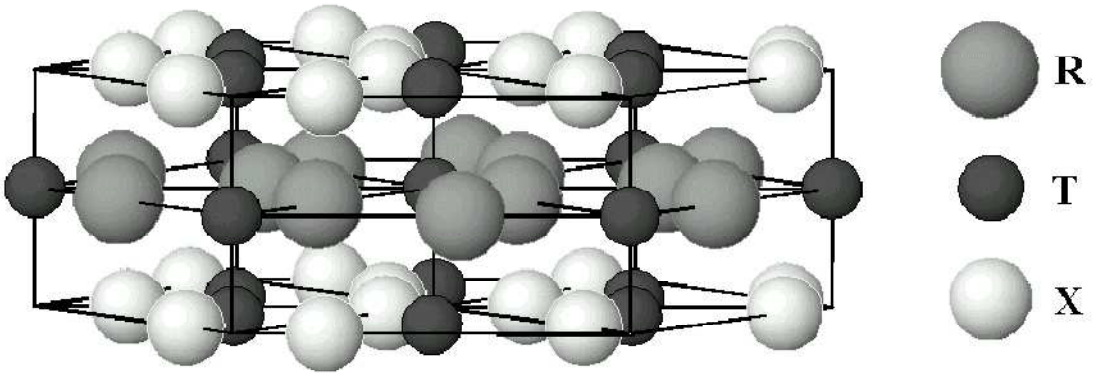

Figure 2.2.1a: ZrNiAl-type hexagonal structure

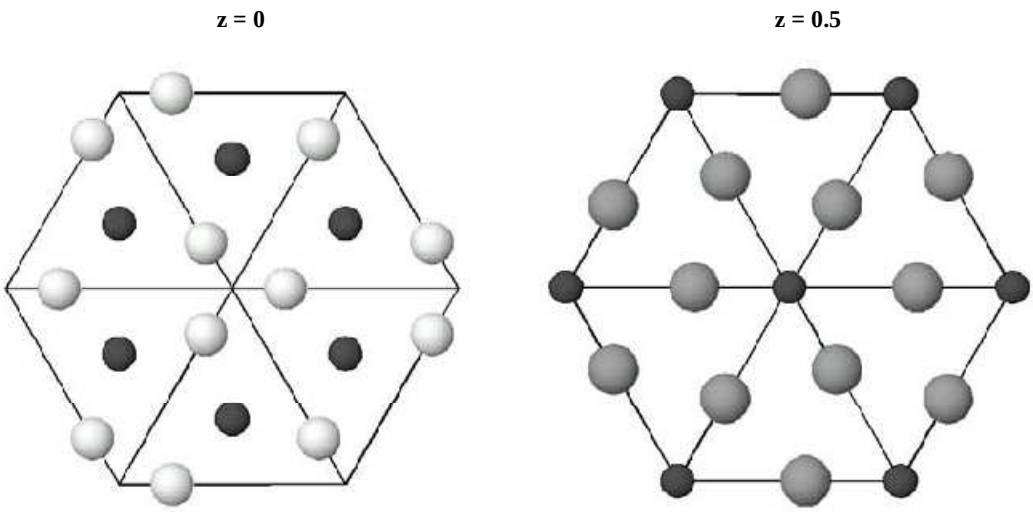

Figure 2.2.1b: Two types of basal planes in ZrNiAl-type structure

There are two types of planes in the ZrNiAl-type hexagonal structure (see Figures 2.2.1a, 2.2.1b). One of the basal planes consists of the rare earth atom (R) and one out of three of the transition metal atoms (T). Another (non-magnetic) layer consists of p-metal (X) and two out of the three transition metal atoms (T). These two planes alternate periodically in the ABAB… sequence.
The coordinates of the elements are following:

3g (R) : (X_R, 0, ½), (0, X_R, ½), (-X_R, -X_R, ½)
1b (T) : (0, 0, ½)
3f (X) : (X_{Al}, 0, 0), (0, X_{Al}, 0), (-X_{Al}, -X_{Al}, 0)
2c (T) : (⅓, ⅔, 0), (⅔, ⅓, 0)

While the positions of transition-metal atoms are fixed, the positions of rare-earth and p-metal atoms depend on internal structure parameters X_R and X_{Al}.

As it can be seen from the Figures 2.2.1a and 2.2.1b, each of the R atoms has four nearest neighbours of the similar element in the same basal plane at a distance

$$d = a\sqrt{1 - 3X_R + 3X_R^2} \qquad (1)$$

Another two neighbours lie in the nearest plane of the same type at a distance of the lattice constant c. Since the transformation involves slight changes of the atomic coordinates X_R a X_{Al}, the nearest neighbours of the R atoms lie also after the change within the basal plane.

2.3 X-ray powder diffraction

Scattering occurs when electromagnetic radiation interacts with matter. The interaction can be either elastic or inelastic. The elastic scattering means that the outgoing rays have the same energy as the incoming rays. Diffraction occurs when the radiation interacts with a periodically arranged system, which period is about the same order as the wavelength of the radiation. If the wavelengths are in the range in the range of 10 to 0.01 nm we talk about an X-ray diffraction. By contrast, inelastic scattering occurs when energy is transferred from the incoming X-ray to the crystal, e.g., by exciting an inner-shell electron to a higher energy level. In our study, we used the elastic scattering, which is useful for determining crystal structure of matter.

In this experiment we worked with Bragg-Brentano geometry. Detailed description of this method can be found for example in [14]. The positions of the diffraction peaks are determined by the Bragg's law of diffraction

$$\lambda = 2d_{hkl} \sin\theta \qquad (2)$$

Where λ stands for wavelength, d_{hkl} is the distance of reflecting inter atomic planes and θ is the angle between the incident ray and surface of the sample.

In the powder diffraction is used to include every possible orientation of the crystallites of the polycrystalline sample.

Powder diffraction data are usually presented as a diffractogram in which the diffracted intensity I is shown as a function of the scattering angle 2θ. Widespread use of powder diffraction is in the identification and characterisation of crystalline solids, each of which produces a distinctive diffraction pattern. Both the positions and the relative integrated

intensity of the lines are indicative of a particular phase and material. In multi-phase mixture, the resulting pattern is a superposition of the phase-patterns, allowing us to determine the relative concentration of the phases in the sample.

3 Experimental methods

3.1 Preparation of the samples

The exact amounts of the elements have been prepared according to the stoichiometric ratio calculations.

The quality of the elements used was as following:

Ce – 3N (3N means that at least 99.9 % of the sample contains Ce)

Al – 5N

Y – 3N

Pd – 3N

The initial mixtures were melted by the mono-arc furnace, installed at Department of condensed matter physics (DCMP), under the protection of an Ar atmosphere (6N) at a pressure of 50 kPa after a previous vacuum of 0.5-2 Pa. Each of the samples was melted and turned 5 times to ensure that the samples will be homogenous. After each melting the weight of the sample was checked to verify that there were not any unexpected looses of material.

3.2 X-ray diffraction

3.2.1 Room temperature X-ray diffraction

Room temperature experiment was realized on the X-ray diffractometer Seifert XRD7, installed at DCMP. This device is dedicated for experiments at room temperature. The device works with Bragg-Brentano geometry. The patterns were measured in the angular range of 2θ from 10° to 120° with chosen resolution 0.04°. The radiation used was generated by the Cu-type lamp with selected wave-lengths $\lambda(K_{\alpha 1})$=1.5401Å, $\lambda(K_{\alpha 2})$=1.5445Å. The sample holder was a glass plate.

3.2.2 High temperature X-ray diffraction

High temperature experiment was realised using the X-ray diffractometer Siemens D500 (also installed at DCMP), which is able to measure under variable temperature conditions

in the range from 3K to 500K. The device works with Bragg-Brentano geometry and its angular resolution is 0.05°. The radiation used is the Co-type with wavelengths $\lambda(K_{\alpha 1})$=1.7889 Å, $\lambda(K_{\alpha 2})$=1.7928Å. The sample holder was a monocrystalline Si plate. The sample space was protected by a mylar cover and evacuated to ensure temperature stability. The data were obtained using positive sensitive detector.

3.2.3 Data analysis

All the measured patterns were analyzed by the FullProf program [15], which enables to refine data from X-ray scattering by the Rietveld method [16]. The structural parameters are refined from positions and intensities of the observed peaks. The analysis of the data was made with corrections on the instrumental deviations.

4 Results and discussion

4.1 Samples preparation

We prepared three samples by the methods described in the paragraph 3.1:

$Ce_{0.8}Y_{0.2}PdAl$

$Ce_{0.5}Y_{0.5}PdAl$

$Ce_{0.2}Y_{0.8}PdAl$

Small amount (≈ 1 % of the calculated weight) of the element Al was added to compensate for evaporation during the melting.

The weights of the compounds were as following:

Table 4.1: Weights of samples

	weight (g)
$Ce_{0.8}Y_{0.2}PdAl$	4.4399
$Ce_{0.5}Y_{0.5}PdAl$	3.1595
$Ce_{0.2}Y_{0.8}PdAl$	3.5945

4.2 Room temperature results

After the preparation of the samples we analysed them on the Seifert X-ray device to verify their quality, crystal structure and to check the agreement with quality of samples previously studied [13]. The data were refined using the FullProf program [15]. These data for all three samples are shown in the Figures 4.2.1, 4.2.2, 4.2.3. The hexagonal ZrNiAl-type structure was conformed using the FullProf program.

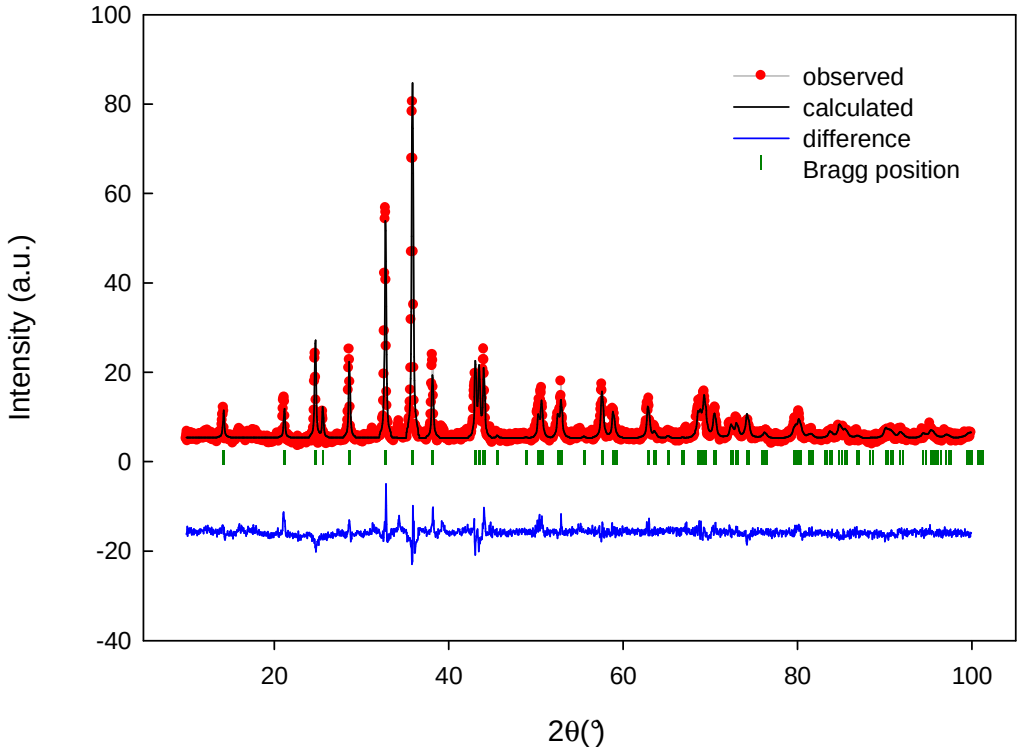

Figure 4.2.1: The X-ray diffraction pattern of $Ce_{0.8}Y_{0.2}PdAl$ sample measured at room temperature using the Seifert device. The red points are observed relative intensities, black line is their refinement. We can see, that they are in good agreement.

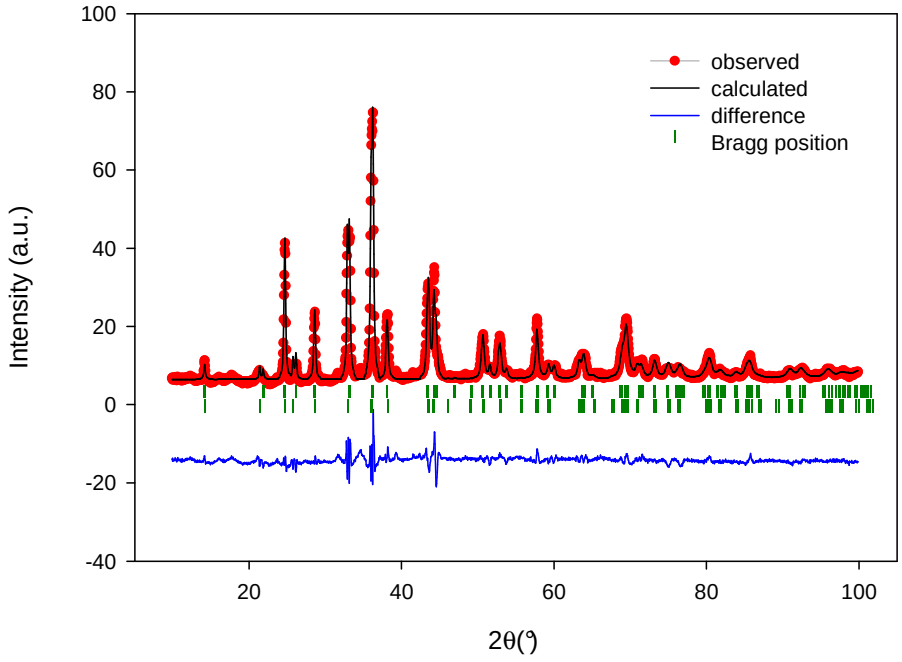

Figure 4.2.2: The X-ray diffraction pattern of $Ce_{0.5}Y_{0.5}PdAl$ sample measured at room temperature using the Seifert device. The red points are observed relative intensities, black line is their refinement. We can see, that they are in good agreement.

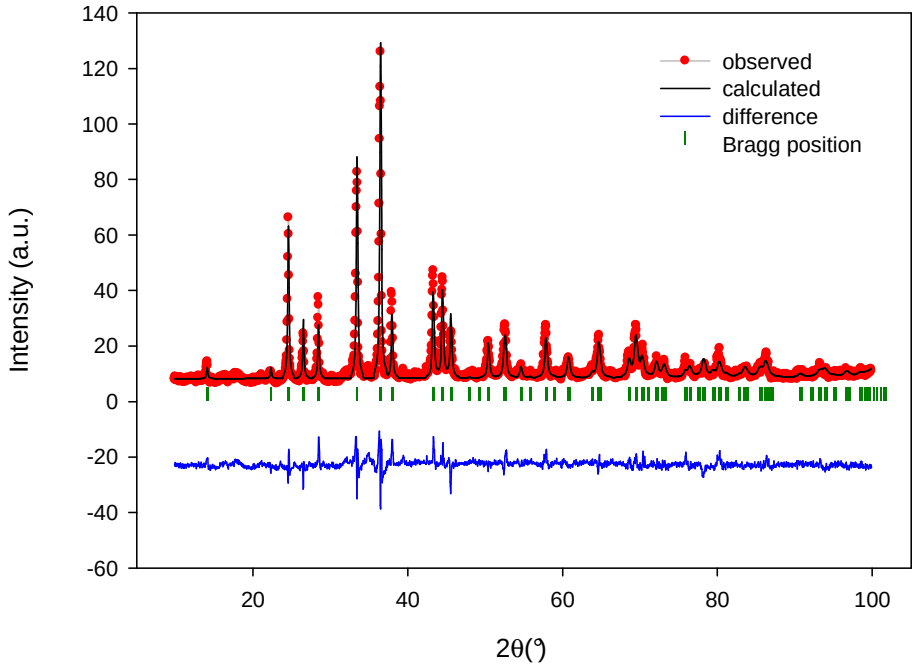

Figure 4.2.3: The X-ray diffraction pattern of $Ce_{0.2}Y_{0.8}PdAl$ sample measured at room temperature using the Seifert device. The red points are observed relative intensities, black line is their refinement. We can see, that they are in good agreement.

As can be seen from careful study of the Figures 4.2.4 and 4.2.5, the $Ce_{0.8}Y_{0.2}PdAl$ and the $Ce_{0.2}Y_{0.8}PdAl$, both exhibit single-phase pattern. The $Ce_{0.5}Y_{0.5}PdAl$ sample seems to have splitting peaks that correspond both with the $Ce_{0.8}Y_{0.2}PdAl$ and $Ce_{0.2}Y_{0.8}PdAl$ peaks. This fact leads to estimation of presence of two different phases of ZrNiAl-type with different values of c and a constants. Fitting of the pattern of $Ce_{0.5}Y_{0.5}PdAl$ with this model of two phases gives a good agreement as can be seen from Figure 4.2.2. Based on previously studied $Ce_{1-x}Y_xPdAl$ series at room temperature [13] we confirm the two-phase state of $Ce_{0.5}Y_{0.5}PdAl$ compound.

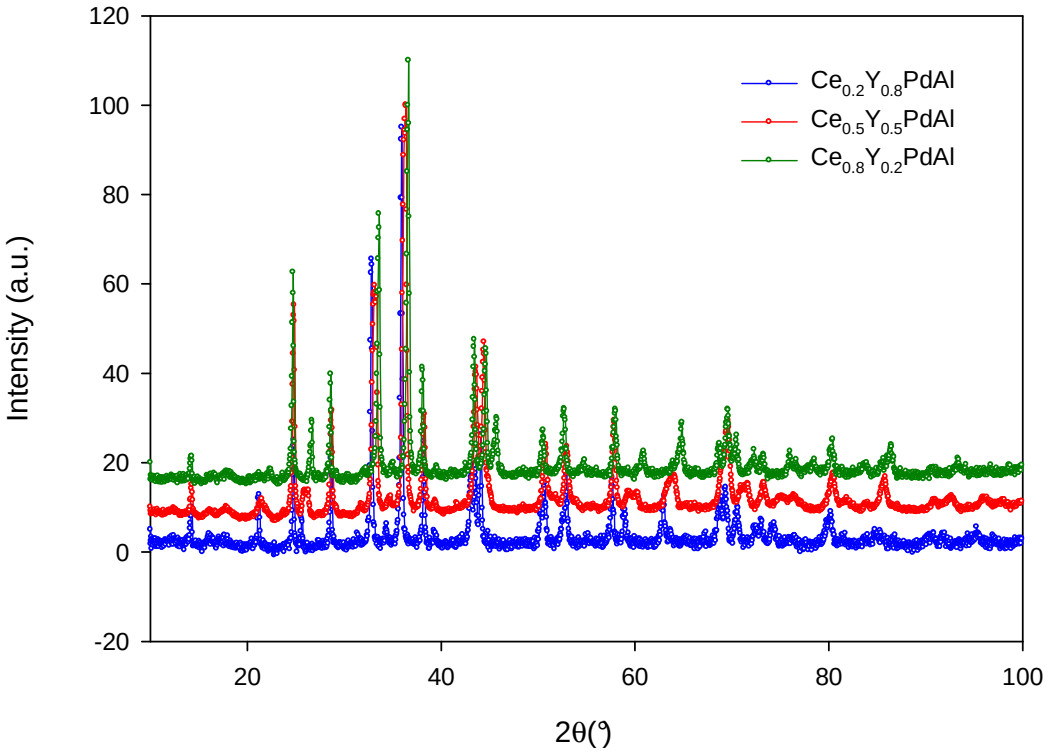

Figure 4.2.4: The X-ray diffraction patterns of all three samples. The relative intensities were shifted so the differences in the diffraction pattern can be better visible. Details of the peaks are show in the next Figure 4.2.5.

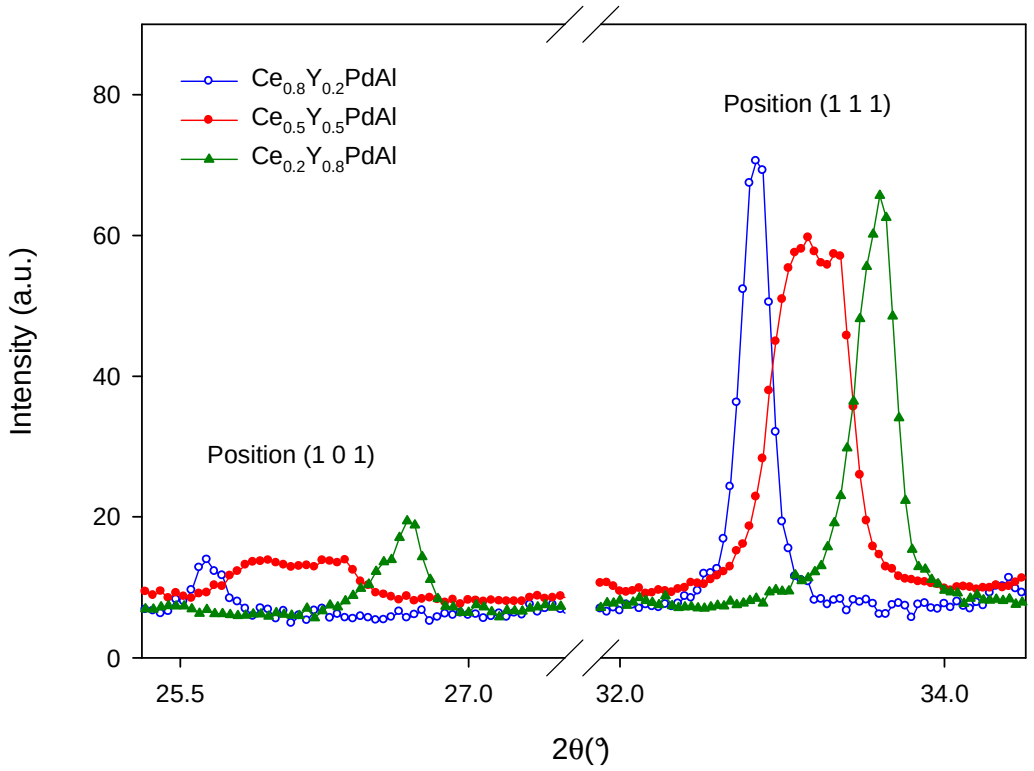

Figure 4.2.5: Details of the peaks form the X-Ray patterns, which shows splitting of the peaks of the $Ce_{0.5}Y_{0.5}PdAl$ sample. The $Ce_{0.8}Y_{0.2}PdAl$ and $Ce_{0.2}Y_{0.8}PdAl$ both exhibit different single phases.

Lattice parameters refined by the FullProf program and their uncertainties are listed in the Table 4.2.1

Table 4.1: Lattice parameters

	a(pm)	c(pm)	c/a	Bragg
$Ce_{0.2}Y_{0.8}PdAl$	723.83 (17)	398.00 (10)	0.54985 (27)	10.9
$Ce_{0.5}Y_{0.5}PdAl$ phase 1	722.28 (19)	406.64 (14)	0.56300 (34)	10.1
$Ce_{0.5}Y_{0.5}PdAl$ phase 2	719.85 (22)	415.25 (17)	0.57686 (40)	7.73
$Ce_{0.8}Y_{0.2}PdAl$	720.55 (18)	419.96 (11)	0.58283 (30)	15.0

To illustrate the transition from single-phase state in $Ce_{0.8}Y_{0.2}PdAl$ to another single-phase state in $Ce_{0.2}Y_{0.8}PdAl$ we show the evolution of the a, c, a/c parameters depending

on the x value (where x is given by $Ce_{1-x}Y_xPdAl$) in the Figure 4.2.6. There are also plotted data from previous experiments [13].

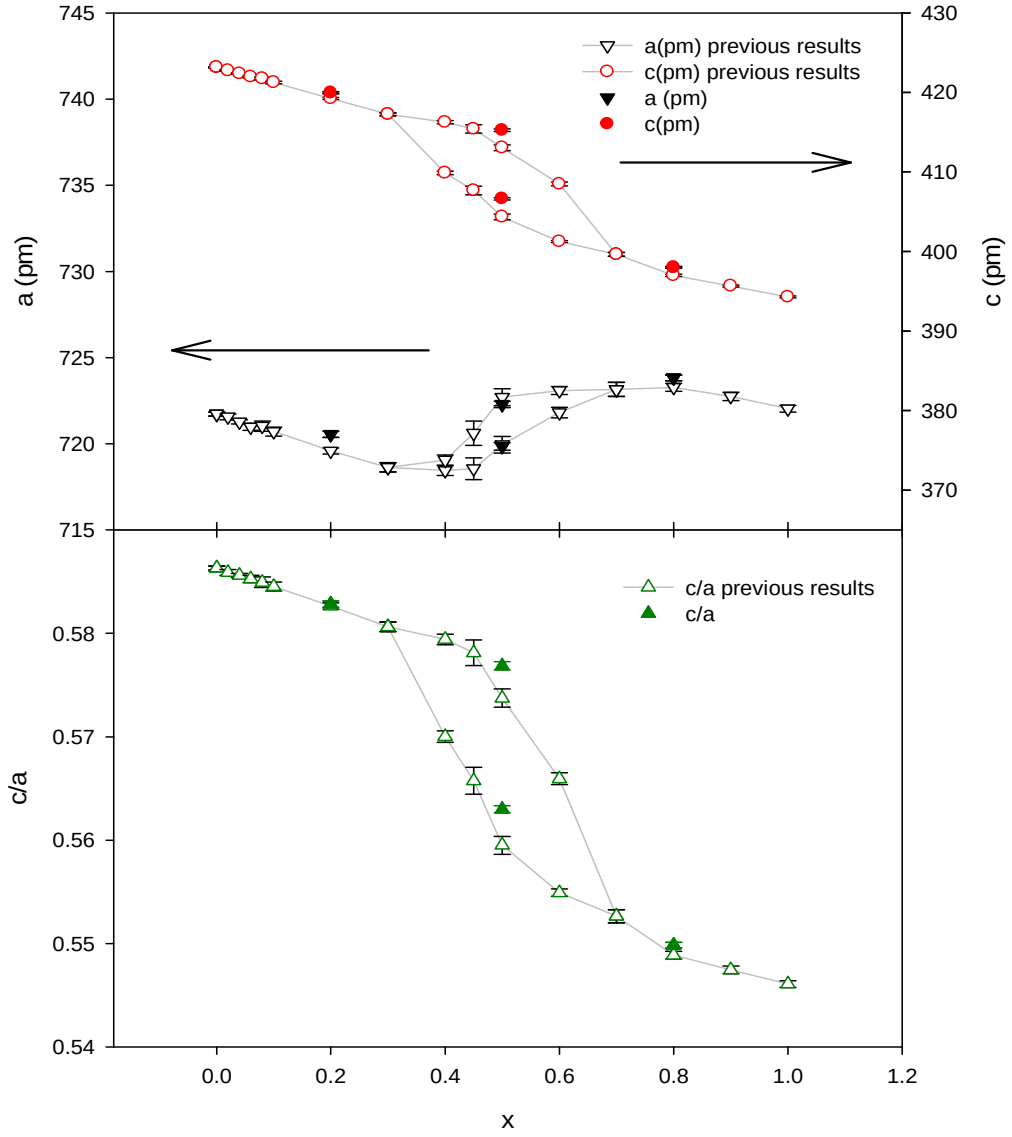

Figure 4.2.6: Evolution of parameters a, c, c/a in dependence on concentration. Sample $Ce_{0.5}Y_{0.5}PdAl$ contains two phases with different a and c.

As can be seen from Figure 4.2.6 the calculated data correspond with the previous experimental results. $Ce_{0.8}Y_{0.2}PdAl$ is in high c/a phase state on the other hand $Ce_{0.2}Y_{0.8}PdAl$ is in low c/a phase state. In the $Ce_{0.5}Y_{0.5}PdAl$ coexistence of both phases was confirmed.

4.3 Temperature scan results

Due to unexpected conditions, the device stopped working durring the experiment, we were able to measure only one sample in the temperature range from 297K to 500K. The sample we chose was the $Ce_{0.5}Y_{0.5}PdAl$ one, because in this compound we expected disappearance of one of the phases with temperature change.

We used the Siemens X-ray device as described in the section 3.2.2. Firstly, we measured powder diffraction on the sample at the temperature of 300K to check agreement of results obtained by the Seifert and Siemens devices.

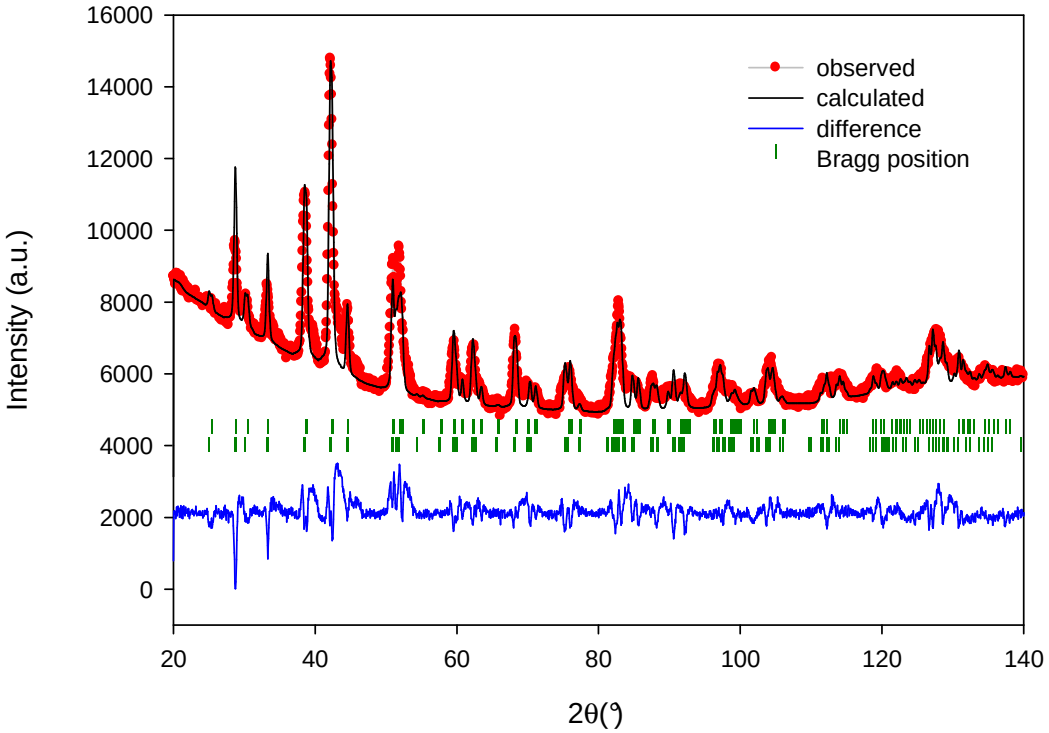

Figure 4.3.1: The X-ray diffraction pattern of $Ce_{0.5}Y_{0.5}PdAl$ sample at 300K in angular range 2θ from 20° to 140° using Siemens device. Measured once.

It's obvious that the data from Siemens device are of a lower quality. Worse signal vs. background ratio was caused by the use of the two layer sample-space cover. Nevertheless, after careful work we were able to obtain lattice parameters (a_{phase1} = 721.7(3) pm, a_{phase2} = 720.2(3)pm, c_{phase1} = 412.7(2)pm, c_{phase2} = 406.2(2)pm) that correspond within error with the previous results from the room temperature

experiment (a_{phase1} = 722.28(19)pm, a_{phase2} = 719.85(22)pm, c_{phase1} = 406.64(14)pm, c_{phase2} = 415.25(17)pm).

We continued to measure diffraction on the sample in the temperature range from 300K to 500K. The step in the temperature was 25K. To increase statistics we decided to measure the samples repeatedly (1 to 22 times) with smaller angular range of 2θ from 24° to 54°. Positive was that we were able to increase quality of the diffraction pattern on the other hand we had to work carefully when obtaining lattice parameters. This range was selected because here the splitting of several reflections is visible at room temperature.
The refined data from 300K, 375K and 475K are shown in the following Figures 4.3.2, 4.3.3, 4.3.4.

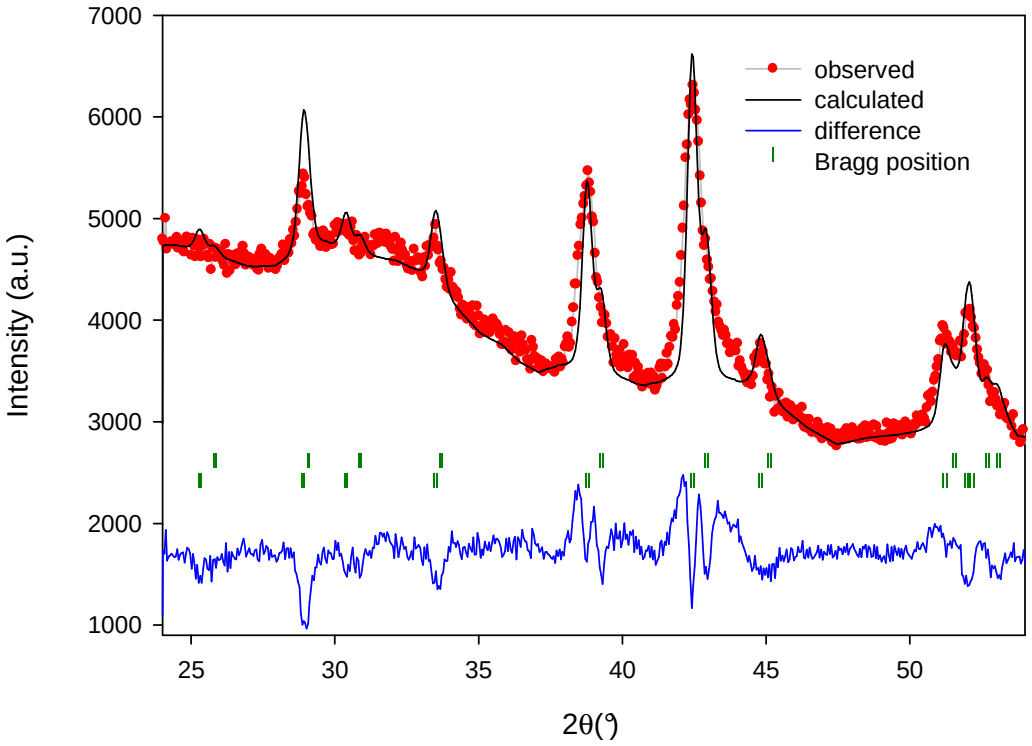

Figure 4.3.2: The X-ray diffraction pattern of $Ce_{0.5}Y_{0.5}PdAl$ sample at 300K using Siemens device. Measured once.

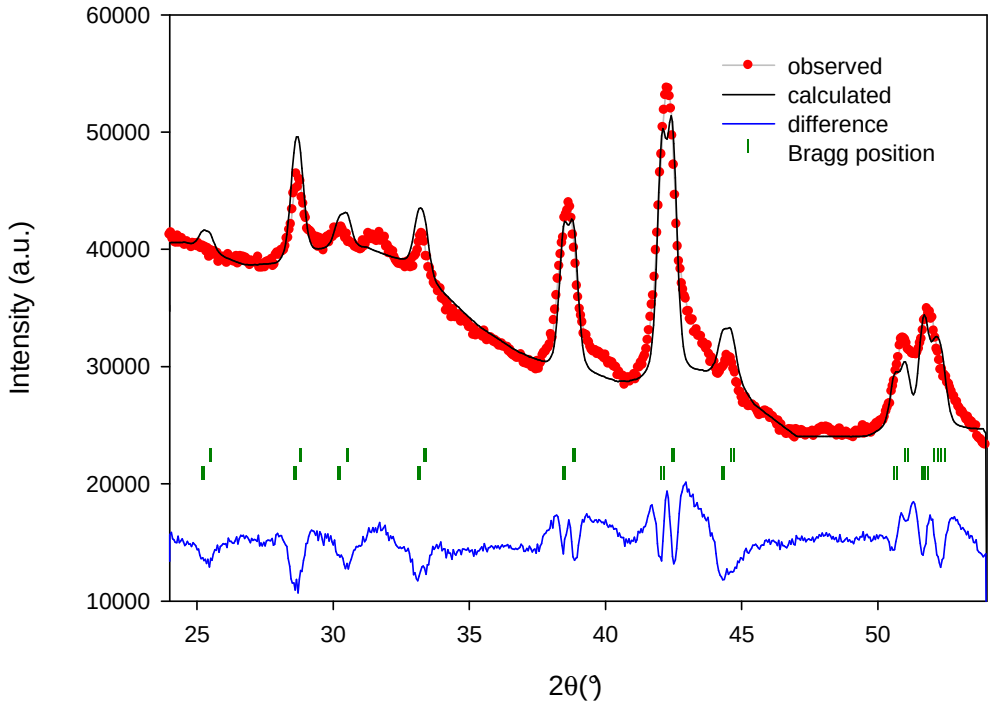

Figure 4.3.3: The X-ray diffraction pattern of $Ce_{0.5}Y_{0.5}PdAl$ sample at 375K using Siemens device. Measured 22 times.

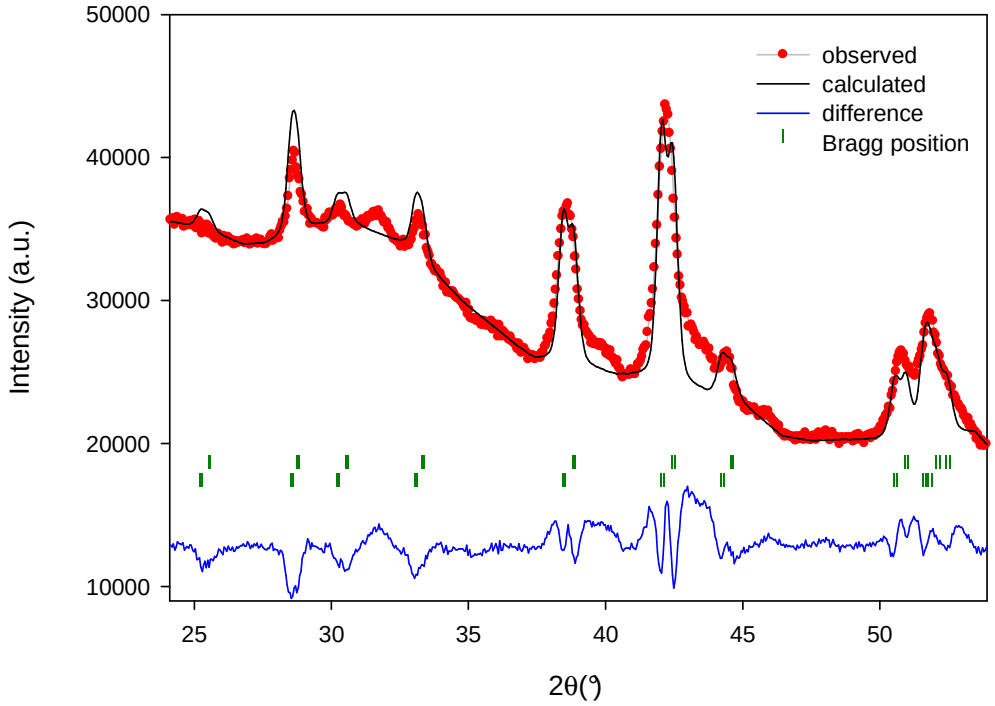

Figure 4.3.4: The X-ray diffraction pattern of $Ce_{0.5}Y_{0.5}PdAl$ sample at 475K using Siemens device. Measured 20 times.

Lattice parameters obtained from these measurements using the Fullprof program and their uncertainties are listed in the Table 4.3.1. The listed R_{Bragg} coefficients are listed to represent similar quality of all the refinements.

Table 4.3.1: Lattice parameters with temperature change.

Temperature (K)		a(pm)	c(pm)	c/a	R_{Bragg}
300	phase 1	720.1 (1.1)	405.3 (0.3)	0.5628 (14)	25.6
	phase 2	722.1 (0.4)	412.7 (0.7)	0.5716 (14)	20.7
325	phase 1	719.5 (1.2)	404.8 (1.0)	0.5626 (23)	25.1
	phase 2	725.1 (0.9)	409.9 (0.8)	0.5653 (18)	20.3
350	phase 1	720.7 (1.1)	405.7 (0.9)	0.5630 (21)	23.7
	phase 2	726.1 (1.0)	410.4 (0.8)	0.5653 (19)	20.3
375	phase 1	721.9 (1.1)	406.4 (0.8)	0.5630 (20)	32.3
	phase 2	727.3 (1.0)	410.8 (0.9)	0.5648 (20)	24.4
400	phase 1	722.1 (1.1)	406.2 (0.9)	0.5625 (21)	26.6
	phase 2	727.4 (1.1)	410.9 (1.0)	0.5649 (22)	18.9
425	phase 1	722.9 (0.9)	406.7 (0.7)	0.5625 (17)	23.6
	phase 2	728.5 (1.0)	411.2 (0.9)	0.5645 (20)	19.2
450	phase 1	723.2 (1.0)	406.5 (0.8)	0.5622 (19)	30.4
	phase 2	728.5 (1.1)	411.3 (1.0)	0.5646 (23)	24.5
475	phase 1	723.3 (1.1)	406.3 (0.9)	0.5617 (20)	28.9
	phase 2	728.9 (0.9)	411.0 (0.8)	0.5638 (19)	22.4
500	phase 1	723.7 (1.4)	406.3 (1.1)	0.5614 (26)	29.1
	phase 2	729.0 (1.4)	411.1 (1.2)	0.5640 (28)	22.2

These data are plotted in the next Figure 4.3.5.

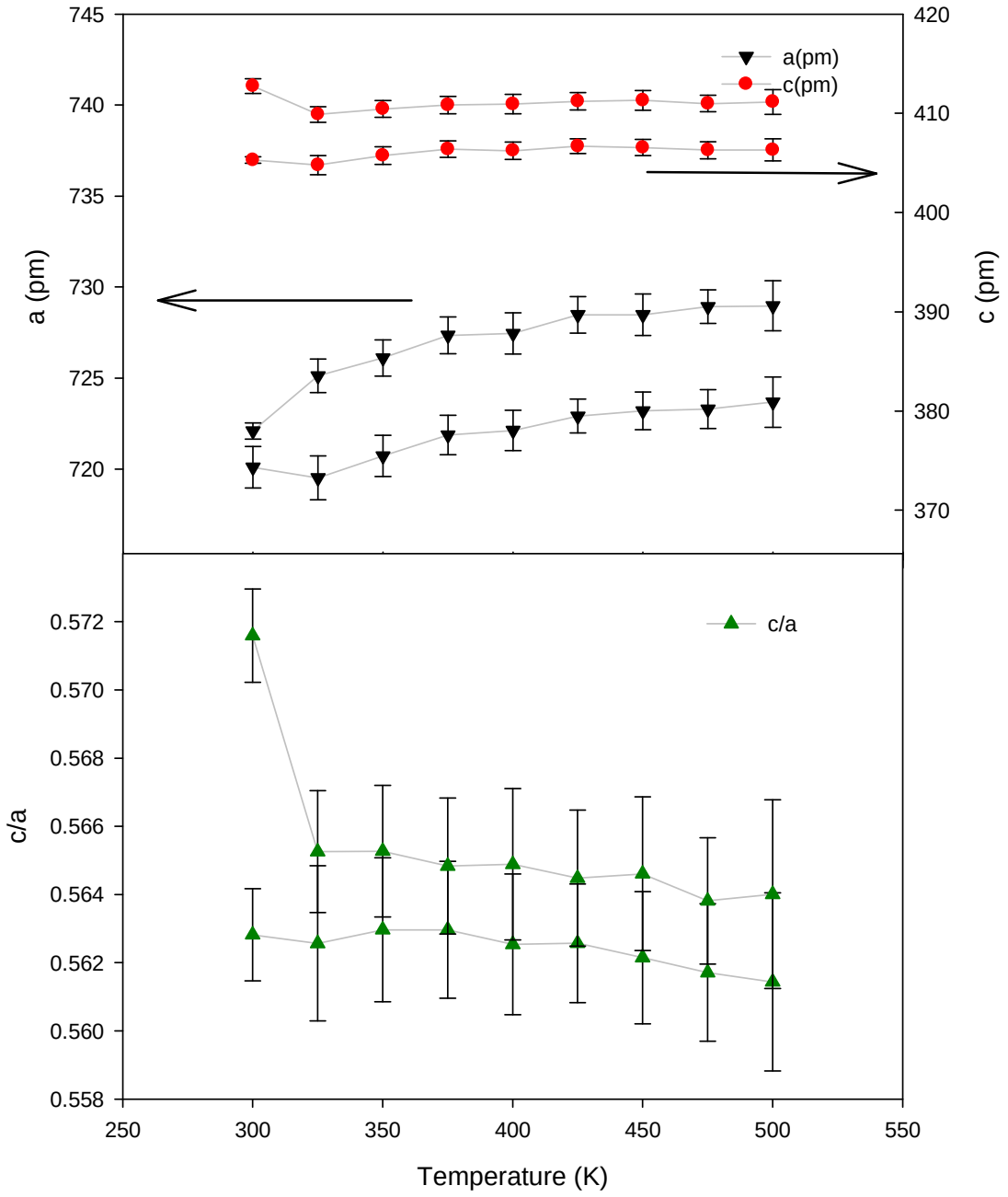

Figure 4.3.5: Evolution of the a, c, c/a ratio in dependence on temperature

To illustrate the evolution of the phase transition we display together measured data from 300K, 375K and 475K diffractions in Figures 4.3.6 and 4.3.7.

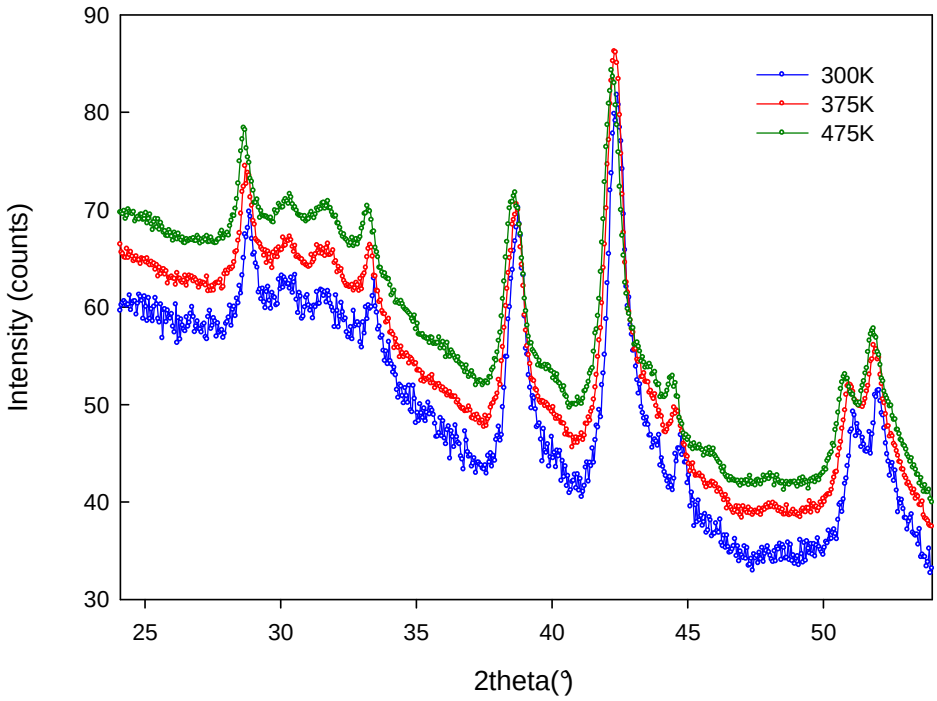

Figure 4.3.6: The X-ray diffraction patterns of $Ce_{0.5}Y_{0.5}PdAl$ sample at 300K, 375K and 475K. The relative intensities were shifted by 5 a.u. so the differences in the diffraction pattern would be better visible.

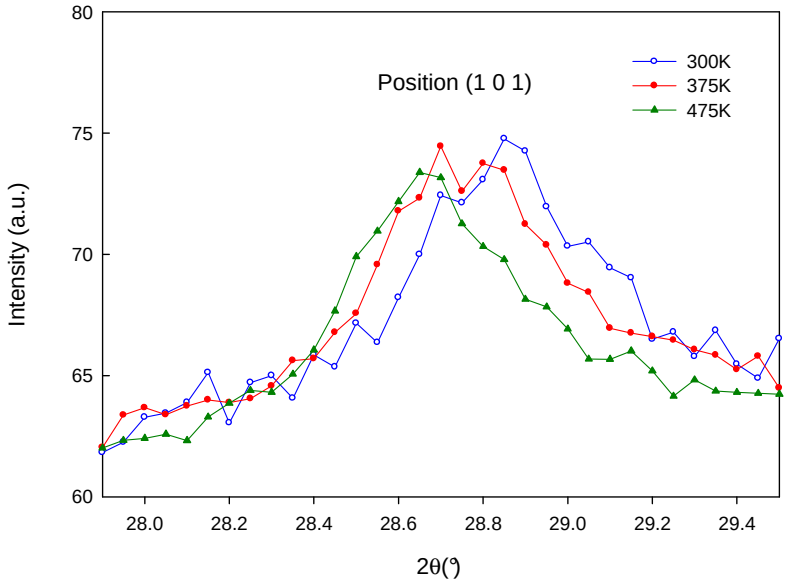

Figure 4.3.7: Details of the peak (1 0 1) from the X-ray diffraction patterns of the $Ce_{0.5}Y_{0.5}PdAl$ sample at 300K, 375K and 475K

If we carefully study the Figure 4.3.5 we may notice trend in the evolution of the c/a ratio. At 300K the high c/a and low c/a values are different but with increasing temperature they are getting closer to each other. This may be caused by disappearing of one of the phases. This conclusion is also supported by the detailed view of the peaks of the (1 0 1) reflection at temperatures 300K, 375K and 475K as shown in the Figure 4.3.7. If we take a closer look we may see that at 300K there are visible both phases, one of them seems to be more populated than the other one. At 375K their roles get changed. At 475K it seems that one of the phases disappears.

The phase transition does not have to be finished at 350K as may seem from the c/a ratio evolution. One of the phases may just consequently become too weak to be distinguished by our device. Nevertheless the trend of disappearing of one of the phases is evident.

5 Conclusion

$Ce_{1-x}Y_xPdAl$ is a hexagonal ZrNiAl-type structure. For x = 0.2 the material is in the "low c/a" phase, for x = 0.8 in the "high c/a" phase, for x = 0.5 there is a coexistence of both phases. These results correspond with the results obtained for this type of compound in the previous work [13].

$Ce_{0.5}Y_{0.5}PdAl$ sample is a two-phased compound at room temperature. According to the high temperature experiment we may conclude that with increasing temperature one of the phases starts to disappear and the other one gets more populated. At higher temperatures one of the phases disappears and the compound seems to be single phased. This is supported either by visual study of the diffraction patterns and also by the calculations of the lattice parameters.

Future view

High and low temperature X-ray scattering experiments are planned for all three samples. A proposal has been submitted for a low temperature X-ray scattering experiment on the $Ce_{1-x}Y_xPdAl$ (x = 0.2, 0.5, 0.8) compounds in National Institute for Material Science in Tsukuba, Japan.

6 References

Reference List

[1] F.Merlo, S.Cirafici, F.Canepa, Journal of Alloys and Compounds 266 (1998) 22-25.

[2] J.Jarosz, E.Talik, T.Mydlarz, J.Kusz, H.Böhm, A.Winiarski, Journal of Magnetism and Magnetic Materials 208 (2000) 169-180.

[3] E.Talik, M.Skutecka, J.Kusz, H.Böhm, J.Jarosz, T.Mydlarz, A.Winiarski, Journal of Alloys and Compounds 325 (2001) 42-49.

[4] G.Ehlers, H.Maletta, Zeitschrift für Physik B 99 (1996) 145-150.

[5] G.Ehlers, D.Ahlert, C.Ritter, W.Miekeley, H.Maletta, Europhysics Letters 37 (1997) 269-274.

[6] J.Prchal, P.Javorský, V.Sechovský, M.Dopita, O.Isnard, K.Jurek, Journal of Magnetism and Magnetic Materials 283 (2004) 34-45.

[7] H.Kitazawa, J.Prchal, N.Tsujii, M.Imai, G.Kido, 2006, pp. 803-804.

[8] G.Ehlers, Frustrierte magnetische 4*f*-Momente in intermetallischen Verbindungen der Lanthaniden, die in der ZrNiAl-Struktur kristallisieren; doctoral thesis, Berlin, 1997.

[9] A.Dönni, H.Kitazawa, P.Fischer, F.Fauth, Journal of Alloys and Compounds 289 (1999) 11-17.

[10] J.Kusz, H.Böhm, E.Talik, M.Skutecka, J.Deniszczyk, Journal of Alloys and Compounds 348 (2002) 65.

[11] J.Prchal, H.Kitazawa, T.Furubayashi, P.Javorský, K.Koyama, V.Sechovský, Physica B 378-380 (2006) 1102-1104.

[12] J.Prchal, P.Javorský, H.Kitazawa, F.de Boer, M.Diviš, J.Rusz, A.Dönni, S.Daniš, V.Sechovský, Physical Review B 77 (2008) 134106.

[13] J.Prchal, H.Kitazawa, O.Suzuki, Journal of Alloys and Compounds 437 (2007) 117-119.

[14] V.Valvoda, M.Polcarová, P.Lukáè, Základy strukturní analýzy, Karolinum, Praha, 1992.

[15] J.Rodriguez-Carvajal, Physica B 192 (1993) 55-69.

[16] H.M.Rietveld, Journal of Applied Crystallography 2 (1969) 65.